Harmonising Force-based and Displacement-based Design Approaches for the Next Generation of Eurocode 8: Application to Reinforced Concrete Moment Resisting Frames

João Pacheco de Almeida [1)*], Sammy De Visscher [2)], Humberto Varum [3)] and António A. Correia [4)]

[1)*] Assistant Professor. Institute of Mechanics, Materials and Civil Engineering, UCLouvain, Louvain-la-Neuve, Place du Levant 1, 1348 Louvain-la-Neuve, Belgium. Tel: +32 10 47 21 23, E-mail: joao.almeida@uclouvain.be, ORCID: 0000-0001-6299-6593

[2)] Undergraduate student. Louvain School of Engineering, UCLouvain, Louvain-la-Neuve, Place du Levant 1, 1348 Louvain-la-Neuve, Belgium.

[3)] Professor. CONSTRUCT-LESE, Faculdade de Engenharia da Universidade do Porto, Porto, Portugal.

[4)] Assistant Researcher. National Laboratory for Civil Engineering (LNEC), Lisbon, Portugal.

Keywords: *Eurocode 8, Force-based design, Displacement-based design, Behaviour factor, Overstrength, Redundancy, Energy dissipation, Reinforced concrete, Moment resisting frame, Chord rotation.*

Abstract

One of the noteworthy developments for the next generation of Eurocode 8 is the inclusion of a complete displacement-based design approach using nonlinear static or dynamic analyses and a set of verifications at the global or local levels, depending on the structural typology. This work investigates the consistency between such approach and classical force-based design applying behaviour factors, for reinforced concrete moment resisting frames. A set of structures designed according to the rules of the three novel ductility classes are used as case studies. Nonlinear static analyses are performed according to a new bilinearisation procedure, and target displacements are computed for the limit states of damage limitation, significant damage, and near collapse. The resulting structural demand, determined globally and in terms of the maximum local deformations among the members, is compared with the recommended values for global and local displacement capacities. Two alternative methods are then used to compute the components of the behaviour factor, which are critically confronted with the currently suggested upper-bound values for design. Finally, a procedure to harmonise displacement-based and force-based approaches is outlined, aiming at deriving values for the design behaviour factor that depend not just on the ductility class but also on additional design parameters which this investigation shows to influence the response.

1 Introduction

Throughout the last decades, the accumulation of a large set of experimental reinforced concrete (RC) member tests has allowed for the derivation of reliable models for their displacement capacity. At the same time, the current availability of engineering numerical models for the simulation of nonlinear seismic response of RC structures allows for increasingly accurate estimates of the displacement demand in their members. Together, these observations are pushing building codes to include and regulate "displacement-based (DB) approaches" in design and assessment of structures. This is one of the key changes included in the next generation of Eurocode 8 (prEN 1998-1-1:2022) [1] with respect to the current generation (EN 1998-1:2004) [2], which is under development for expected release around the middle of the present decade. Such displacement-based approach to determine the seismic action effects in a structure is offered as an alternative to the currently available "force-based (FB) approach". The FB design method, familiar to all design engineers in the many countries adopting the Eurocodes, as well as most other seismic design codes, employs a linear analysis that implicitly accounts for the overstrength and the nonlinear response through a behaviour factor, and performs verifications in terms of forces. It is implemented in the form of a static lateral force method or a response spectrum method of analysis. The new displacement-based approach is not a strict direct DB design approach [3] (i.e. engineers will still be constrained to employ a FB approach for preliminary design) but rather a method for analysis, verification and assessment that explicitly accounts for the structural nonlinear response through pushover calculations and employs verifications in terms of displacements or deformations. Since the next-generation Eurocode 8 (EC8) will offer these alternative FB and DB verification methods, with potential significant implications in terms of engineering practice and economic impact, it becomes of utmost relevance to assess and calibrate their relative safety level. The objective of the current investigation is to address this issue, using as case studies several buildings with frame systems, which in prEN 1998-1-2:2022 [4] are named moment resisting frame structures (i.e. spatial frames whose shear resistance at the building base exceeds 65% of the total shear resistance of the whole structural system). For the sake of completion, it should be mentioned that prEN 1998-1-1:2022 [1] allows for another DB design and assessment option which consists in using response-history analyses.

The following section analyses some aspects of FB and DB design in the context of the prEN 1998-1-1:2022, with particular focus on the displacement-based approach. Some preliminary information, required to understand the rest of the work, will also be introduced. Section 3 briefly describes the design of the case-study frames, highlighting the major aspects of novelty specific to the next code generation, and Section 4 sums up the results of the corresponding nonlinear static analyses. Section 5 proposes and applies two methods to determine the components of the behaviour factor, and discusses critically the results of the analyses against the currently proposed coefficients regulating global and local DB verifications. Finally, Section 6 discusses the influence of the design parameters in the local plastic deformation demands and proposes a harmonisation procedure to determine consistent behaviour factors in force-based design.

2 Force-based and displacement-based design in the next-generation Eurocode 8

2.1 Overview

The force-based and displacement-based approaches of prEN 1998-1-1:2022 [1] are performance-based methodologies, common in all advanced codes worldwide [5], meaning that different limit states (LS) are associated to different seismic action levels and consequence classes (CC1 to CC3; similar to importance classes in the current version). The LS of 'near collapse' (NC) and of 'significant damage' (SD) can be considered Ultimate Limit States, whereas the LS of 'damage limitation' (DL) and 'fully operational' (OP) should be considered Serviceability Limit States. The attainment of performance requirements should be achieved by selecting appropriate return periods, depending on the specified limit state and consequence class. An alternative basic representation of the seismic action is adopted in prEN 1998-1-1:2022 [1]: instead of anchoring the horizontal response spectrum to a design ground acceleration a_g and two types of spectra, as it is currently established, the elastic response spectrum for horizontal components will be based on a single spectrum type defined by the spectral accelerations S_α and S_β. S_α corresponds to the maximum response spectral acceleration at the constant acceleration range, whereas S_β corresponds to the spectral acceleration at the vibration period T_β, equal to 1 s, for 5% damping.

One additional difference between the current and the future versions of the Eurocode 8, of relevance to the current investigation, is the definition of new ductility classes (DC), ordered from DC1 to DC3. In DC1, only the overstrength capacity is considered and it mostly corresponds to the current ductility class DCL, although it can be used up to a higher maximum pseudo-acceleration $S_{\alpha=DC1} = 3\ m/s^2$. DC2 corresponds to moderately ductile structures and takes also into account the local deformation capacity and energy dissipation, while controlling the formation of global plastic mechanisms. Finally, DC3 corresponds to highly ductile structures and considers additionally the ability of the structure to form a global plastic mechanism at the SD limit state. The current ductility class DCH requirements are simplified in prEN 1998-1-1:2022 [1], since experience proved it to be too demanding in terms of design detailing.

2.2 Force-based approach and the components of the behaviour factor

The reduced-spectrum for the next-generation FB design approach – of application for both the lateral forces method and the response spectrum method – is obtained from the elastic response spectrum through introduction of a behaviour factor q, as it is common use. The most notable difference regarding the current version of the Eurocode 8 is the explicit decomposition of the behaviour factor q into three components:

$$q = q_R q_S q_D \tag{1}$$

where q_S accounts for over-design and overstrength (and is taken equal to 1.5 for all DCs and types of structures), q_R is the behaviour factor component reflecting the overstrength due to the redistribution of seismic action effects in redundant structures (=α_u/α_1 in the current version of the Eurocode 8), and q_D is the component accounting for the deformation and energy dissipation capacity.

It is noted that the force-based approach should not be used, in principle, for verification to the NC limit state, but may be used for verification to SD. It may also be used for verifications to DL and OP using $q = 1$ in the analysis. According to prEN 1998-1-2:2022 [4], the upper-bound values of the behaviour factor for multi-storey, multi-bay moment resisting frames, which will be studied in this work, are $q = 2.5$ (DC2) and 3.9 (DC3), corresponding to components $q_R = 1.3$ and $q_D = 1.3$ (DC2) and 2.0 (DC3). For the design of the frames used later as case studies in this investigation, the behaviour factor adopted is denoted q_{design}, instead of q, to emphasize the distinction with computed values of these behaviour factors after nonlinear analysis, as it will be explained.

2.3 Displacement-based approach: changes to the N2 method

The displacement-based approach proposed by the next-generation EC8 [1] requires the use of a realistic nonlinear structural model and a nonlinear static analysis method. The adaptation to the Capacity Spectrum Method-type [6] of nonlinear static procedure known as N2 Method [7], [8] is kept from the current version [2], but it comprises some modifications.

At least a "modal" pattern of loads should be applied for the pushover analysis, i.e. the lateral force applied at a node should be proportional to the product between the nodal mass and the associated displacement at the vibration mode corresponding to the largest value of the effective modal mass for the considered direction of seismic action. The resulting capacity curve of the multi-degree-of-freedom structure should plot the total base shear F_b *versus* the control displacement d_n (which should be selected as the node where the vibration mode has the largest component, usually the top floor for buildings). The pushover analysis should progress until a displacement d_u where an ultimate local deformation in a ductile post-elastic mechanism is attained, or brittle failure, whichever occurs first. Using well-known transformation relations [8], the curve $F_b(d_n)$ should then be converted into a force-deformation relationship of an equivalent single-degree-of-freedom (SDoF) system, $F^*(d^*)$.

A notable difference between the current and the next EC8 generations regards the bilinearisation of the capacity curve. Whereas in the present version an idealised elastic-perfectly plastic force-displacement relationship is considered, for prEN 1998-1-1:2022 [1] the $F^*(d^*)$ relation may be always idealised as bilinear if the capacity curve is non-decreasing, see Figure 1(a). If the capacity curve exhibits a peak and a post-peak negative stiffness branch (e.g. due to geometric nonlinearities and/or member strength degradation), see Figure 1(b), the bilinear idealisation may be adopted up to the peak for design purposes. Point A in Figure 1, with coordinates (d_1^*, F_1^*), corresponds to the first plastic hinge formation in the structure, which is intended to indicate the first yield chord rotation θ_y attained in one element in the structure. This point defines the slope of the elastic region, characterised by an equivalent stiffness $k^* = F_1^*/d_1^*$. Point B corresponds to the maximum force and has coordinates (d_m^*, F_m^*). Finally, the plastification or yield point (d_y^*, F_y^*) is computed such that the dissipated energy E^* up to the maximum displacement d_m^*, under the real curve and the bilinear idealisation, is identical. The displacement d_y^* can therefore be obtained:

$$d_y^* = \frac{2E^* - F_m^* d_m^*}{k^* d_m^* - F_m^*} \quad (2)$$

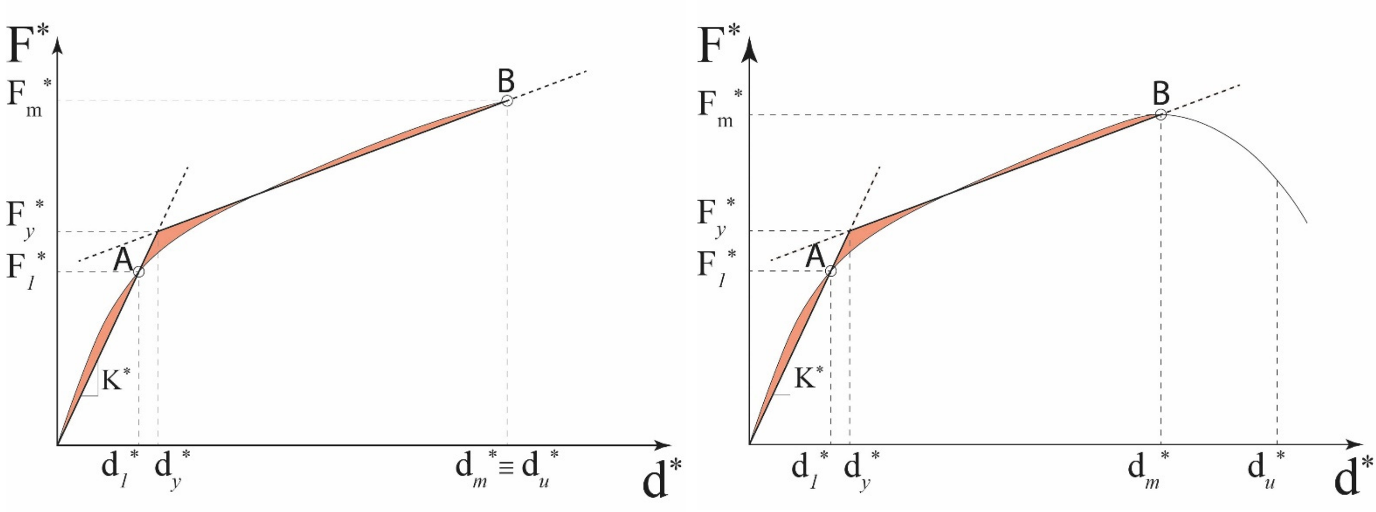

(a) (b)

Figure 1. Bilinear idealisations of the capacity curve for: (a) non-softening response, and (b) response with a post-peak softening branch.

Finally, the determination of the target displacement, also known as performance point, requires the conversion of the bilinear SDoF force-displacement curve into a bilinear capacity spectrum in the ADRS (acceleration-displacement response spectrum) format. The combination with the elastic response spectrum for the LS under consideration depends on whether the SDoF has an equivalent period T^* smaller or larger than the corner period T_C of the elastic response spectrum. Since the procedure proposed in prEN 1998-1-1:2022 [1] is identical to the one in the current EC8 [2] – in turn inspired from well-known historical developments [9], [10] – no further details are provided herein due to space limitations.

2.4 Displacement-based approach: global and local verifications

The force-based approach in prEN 1998-1-1:2022 [1] employs the usual procedure requiring that action effects in the seismic design situation, expressed in terms of forces, do not exceed the corresponding resistance of the structural elements, $E_d < R_d$. The novel checks concern the verifications associated with the displacement-based approach at the Ultimate Limit States (SD and NC, with SD taken as reference), for which two possibilities arise. For structural types or materials for which local "yield" deformation are given – the prEN 1998-1-1:2022 [1] includes a chapter dedicated to deformation criteria and strength models for materials –

these verifications are performed locally at the member level. When that is not the case, for example for masonry or timber structures, the verifications are carried out globally in terms of displacements of the equivalent SDoF model. The capacity and demand are computed using mean material properties in nonlinear analysis, verification and assessment.

Starting with this latter global verification, the next-generation EC8 proposes the following check for SD:

$$d_{SD}^* \leq d_{SD,limit}^* = \frac{1}{\gamma_{Rd,SD,d}}\left[d_y^* + \alpha_{SD,d}\left(d_u^* - d_y^*\right)\right] \tag{3}$$

where d_{SD}^* is the structural target displacement for SD, $\alpha_{SD,d}$ is the portion of the plastic part of the equivalent SDoF displacement corresponding to the attainment of SD, and $\gamma_{Rd,SD,d}$ is a partial factor on resistance at SD. The displacement d_y^* was defined in the previous section, whereas d_u^* is deduced from the ultimate displacement d_u at the structural level corresponding, in any primary member, to an ultimate local deformation in a ductile post-elastic mechanism, or to a brittle failure or instability when this occurs first. As it currently stands, the reference value defined in prEN 1998-1-1:2022 [1] for $\alpha_{SD,d}$ is equal to 0.35.

For structures where the local member behaviour can be considered as acceptably known and amenable to reliable nonlinear modelling, such as RC or steel structures, the application of the previous global verification will in general produce over-conservative results. In such cases, the following local verification of ductile mechanisms is proposed for SD:

$$\delta_{SD} \leq \delta_{SD,limit} = \frac{1}{\gamma_{Rd,SD,\delta}}\left[\delta_y + \alpha_{SD,\delta}\delta_u^{pl}\right] \tag{4}$$

where δ_{SD} is a local deformation for SD, $\alpha_{SD,\delta}$ is the portion of the plastic part of the ultimate deformation $\delta_u^{pl} = \delta_u - \delta_y$ (computed with mean material properties) that corresponds to the attainment of SD, and $\gamma_{Rd,SD,\delta}$ is a partial factor on resistance at SD. For frame structures, as addressed in this work, δ corresponds to the chord rotation θ, and therefore this latter index is used in the variables that follow, instead of δ. In its current version, the reference value defined in prEN 1998-1-1:2022 [1] for $\alpha_{SD,\theta}$ is equal to 0.5. The partial factor $\gamma_{Rd,SD,\theta}$ at SD depends on the type of structure and it is given as $\gamma_{Rd,SD,\theta} = \gamma_{Rd,k} \cdot s_\gamma$, i.e. as a product of a factor associated to a fractile of resistance k and a shape factor s_γ. Finally, it should be noted that, still within the scope of local verifications in DB approaches, an additional check for brittle mechanisms needs to be performed, which is carried out in terms of strength, e.g. verification of shear resistance in RC members.

2.5 Design of RC moment resisting frames according to the next-generation EC8

This section addresses salient aspects of design rules and requirements for RC moment resisting frames according to the next-generation EC8 [1], [4], contrasting them against the current code generation EN 1998-1:2004 [2]. Due to space constraints, only a very brief overview of the overall structural design process is included, together with some general relevant observations relative to the design of beams, columns, and beam-column joints. The interested reader is forwarded to the work by De Visscher [2021] for further details.

Firstly, and importantly, it is noted that the elastic stiffness to be employed in the numerical models for linear analysis should be equal to the secant effective stiffness referring to the elastic limit of the structural element. For RC structures, it corresponds to that of cracked sections at first longitudinal reinforcement yielding [1], considering mean values of material properties and the presence of axial forces [4]; accurate analyses of the cracked members are allowed to determine the effective elastic flexural and shear stiffness. Otherwise, the code permits to assume one-half of the corresponding stiffness of the uncracked members, or other fractions if defined for the specific typology (type of structure and construction material) and members. From this perspective, considering the provisions of its last version, the next-generation code is similar to the current one [2]. This important point will again be discussed in Section 5.1. It is remarked that many other international codes provide detailed guidance on the value of the effective stiffness as a function of the gross moment of inertia, generally differentiating between the type of structural member (i.e. beams, columns, walls, slabs), and in the case of columns also as a function of the axial load ratio [11]. It is interesting to observe that the next-generation appears to give a first step towards more specific guidance on the elastic stiffness, as expressed in the recommendation of one-third of the uncracked stiffness for flat slabs simulated with equivalent-beam models [4].

A second relevant clause applicable to RC buildings at the SD limit state, which is independent of the ductility class and can control the design of RC frames (see Section 3), is the limitation of the interstorey drift to 2% [4]. In the current code [2] the interstorey drift is also restricted: the limits vary between 0.5% (if brittle non-structural elements are present) and 1% (if the non-structural elements do not interfere in the structural deformations); however, these checks are applicable for damage limitation. It is also noted that the control of the second order effects is performed through an approach that, in essence, is similar between the two code generations, although the newer version is more correct and aligned with the decomposition of behaviour factor components.

It is expected that, for many RC moment-resisting frames of ductility class DC3, the longitudinal reinforcement of the columns will be governed by the “strong column – weak beam” capacity design rules specified in the next-generation code. They should be satisfied at all joints of primary or secondary beams with primary seismic columns, and impose that the sum of the absolute values of the design resisting moments of the columns framing each joint should be 1.3 times higher than those of the beams framing the same joint. For DC2 frames, the future code [4] chose not to impose the previous verification that enforces global plastic mechanisms. Instead, it imposes a different capacity design rule, easier to verify, to mitigate the occurrence of a soft storey plastic mechanism (Section 2.1); it is expressed globally for each storey level and not for each beam-column separately.

Capacity design rules for beams and columns are, as expected, also present in the next-generation code [4]. The latter, which should be employed to compute the transverse reinforcement in order to avoid brittle shear failures, are only required for ductility classes DC2 and DC3, but not for DC1. The verifications are quite similar to the verifications currently required [2].

Regarding beam-column joints, for DC1, the horizontal reinforcement should not be in general smaller than that of the columns framing into the joint. For DC2 and DC3, the minimum confinement reinforcement corresponds to that specified for the critical regions of the columns. Specifically for DC3, and significantly, the new code generation [4] will now include expressions to compute the design shear force acting on the concrete core of the joints (both for exterior and interior beam-column joints), as well as comprehensive guidance on the determination of the corresponding design shear resistance. The above corresponds to a significant evolution with respect to the current code [2].

Many other design detailing requirements have undergone adjustments, in general moving towards a simplification for ductility class DC3 [1] with respect to current DCH in EN 1998-1:2004 [2], as the latter was judged too demanding for design and construction practice. As an example, the maximum spacing of hoops and cross-ties in critical regions of primary seismic columns of DC3 is now similar to that requested presently for DCM, and for DC2 the next-generation code is only slightly more lenient than for DC3.

3 Design of case-study frames with the force-based approach

The case studies considered in the present investigation consist of 28 RC frames. They combine three distinct numbers of storeys (three, five, and eight), two soil types (B and D), four peak ground accelerations (a_g = 0.74 m/s^2, 1.48 m/s^2, 2.22 m/s^2, 2.84 m/s^2), and three ductility classes (DC1, DC2, and DC3), as indicated in Table 1. The latter includes a column referring to the maximum response spectral acceleration at the constant acceleration range S_α (see Section 2.1); the different values for the soil types B and D are due to the distinct soil amplification factors. The table also shows the behaviour factor used for the design of the frames (according to Section 2.2) and the label used for each model, which will be referred throughout the study.

Table 1. Summary of the 28 RC frames designed and analysed as case studies.

Soil Type	No.	Ductility	a_g [m/s^2]	S_α [m/s^2]	q_{design} [-]	Label
B	5	DC3	2.84	8.5	3.9	5S-TypeB-DC3-0,85g
			2.22	6.7	3.9	5S-TypeB-DC3-0,67g
			1.48	4.4	3.9	5S-TypeB-DC3-0,44g
			0.74	2.2	3.9	5S-TypeB-DC3-0,22g
		DC2	1.48	4.4	2.5	5S-TypeB-DC2-0,44g
			0.74	2.2	2.5	5S-TypeB-DC2-0,22g
		DC1	0.74	2.2	1.5	5S-TypeB-DC1-0,22g
D	5	DC3	2.84	9.6	3.9	5S-TypeD-DC3-0,96g
			2.22	7.5	3.9	5S-TypeD-DC3-0,75g
			1.48	5.0	3.9	5S-TypeD-DC3-0,50g
			0.74	2.5	3.9	5S-TypeD-DC3-0,25g
		DC2	1.48	5.0	2.5	5S-TypeD-DC2-0,50g
			0.74	2.5	2.5	5S-TypeD-DC2-0,25g
		DC1	0.74	2.5	1.5	5S-TypeD-DC1-0,25g
B	3	DC3	2.84	8.5	3.9	3S-TypeB-DC3-0,85g
			2.22	6.7	3.9	3S-TypeB-DC3-0,67g
			1.48	4.4	3.9	3S-TypeB-DC3-0,44g
			0.74	2.2	3.9	3S-TypeB-DC3-0,22g
		DC2	1.48	4.4	2.5	3S-TypeB-DC2-0,44g
			0.74	2.2	2.5	3S-TypeB-DC2-0,22g
		DC1	0.74	2.2	1.5	3S-TypeB-DC1-0,22g
B	8	DC3	2.84	8.5	3.9	8S-TypeB-DC3-0,85g
			2.22	6.7	3.9	8S-TypeB-DC3-0,67g
			1.48	4.4	3.9	8S-TypeB-DC3-0,44g
			0.74	2.2	3.9	8S-TypeB-DC3-0,22g
		DC2	1.48	4.4	2.5	8S-TypeB-DC2-0,44g
			0.74	2.2	2.5	8S-TypeB-DC2-0,22g
		DC1	0.74	2.2	1.5	8S-TypeB-DC1-0,22g

The frames have two spans of 6 m each and an interstorey height of 3 m, except for the ground storey whose height is 3.5 m. The spacing between the frames is assumed as 5 m. A concrete class C35/45, following the classification of Eurocode 2 [12], is assumed. The material properties used for the structural design and in Section 4 for the nonlinear analyses are summarised in Table 2. The safety factor for concrete is $\gamma_c = 1.5$ and for steel $\gamma_s = 1.15$. The gravity loads, which respect Eurocode 1 [13] and are modelled as distributed loads along the beams, are also listed in Table 2. The self-weight of the frame members is taken into account directly by the structural analysis software. The seismic loads, represented simply as E, are defined according to the 5% damped spectrum of Type 1 as defined in the current generation of EC8 [2]. A consequence class CC2 according to prEN 1998-1-1:2022 [1] is assumed (equivalent to an importance class II in the current generation [2]), meaning that the design response spectrum does not require amplification.

The building is regular in plan and in elevation: the design is performed with the lateral force method of analysis resorting to a planar model. The structural analyses for this design phase were performed with the software SCIA Engineer. The frame dynamic properties (after final design) show that the applicability conditions for the lateral force method, i.e. $T_1 < min\{4 \cdot T_C; 2.0\ s\}$ (where T_1 is the fundamental period and T_C is the corner period of the response spectrum corresponding to the end of the constant-acceleration plateau), are met except for some 8-storey frames. However, the most flexible of the case-study frames is characterised by $T_1 = 2.16\ s$, i.e. only marginally exceeding the limit of 2.0 s; moreover, the effective modal masses show a very limited contribution of the higher modes. Therefore, this method was applied and the equivalent lateral forces were distributed throughout the height of the frames proportionally to the product of the first modal shape and the storey masses. The fundamental elastic periods T_1 for the several frames are included in Table 3 to Table 6. It is recalled that the elastic pseudo-acceleration corresponding to T_1 is, in the current EC8, multiplied by a factor $\lambda = 0.85$ if $T_1 \leq 2 \cdot T_C$.

Two load combinations for the ultimate limit states are considered in the design of the structure [14]: (i) a fundamental combination, herein called ‘gravity design combination’ for easier understanding, obtained by weighting dead and live loads according to $\gamma_G \cdot G_{k,i} + \gamma_Q \cdot Q_k$, with $\gamma_G = 1.35$ and $\gamma_Q = 1.5$, and (ii) a ‘seismic design combination’, obtained according to $G_{k,i} + \psi_{E,i} \cdot Q_k + E$, with $\psi_{E,i} = 0.3$. The masses were calculated from the gravity loads associated to this latter load combination; the mass of the frame members is considered automatically by the structural analysis software.

Table 2. Summary of the material properties and gravity loads used for the design and analyses of the RC frames.

Materials

Concrete									
f_{ck}	f_{cm}	f_{cd}	f_{ctk}	f_{ctm}	f_{ctd}	E_{cm}	ε_{c1}	ε_{cu1}	ρ_c
[MPa]	[MPa]	[MPa]	[MPa]	[MPa]	[MPa]	[GPa]	‰	‰	$[kg/m^3]$
35	43	23.3	2.2	3.2	1.5	34	2.25	3.5	2500

Steel						
f_{yk}	f_{ym}	f_{yd}	E_s	ε_y	ε_u	ρ_s
[MPa]	[MPa]	[MPa]	[GPa]	%	%	$[kg/m^3]$
500	575	434.8	200	0.25	5	7850

Loads

Dead loads	Self-weight, $G_{k,1}$	All storeys	Columns, Beams	25 kN/m^3
			Slabs (15-cm thick)	
	Other permanent loads, $G_{k,2}$	Current storeys	External walls and partitions [13]	1.2 kN/m^2
			Floor finishing	1.3 kN/m^2
		Roof	Floor finishing	1 kN/m^2
Live loads, Q_k		Current storeys	Floors, Category A [13]	2 kN/m^2
		Roof	Non-accessible roofs, Category	1 kN/m^2

The design of the frames followed the indications in Section 2.5, as well as other more specific ones not discussed in detail. The longitudinal and transverse reinforcement of the members was computed based on the most conditioning design values as obtained from the gravity and the seismic design combinations. For the column design, the axial force-bending moment interaction was considered for the gravity and seismic design combinations (both for positive E^+ and negative E^- directions). The column longitudinal reinforcement was often conditioned by the "strong column – weak beam" capacity design rule specified for DC3, namely for the 3 and 5-storey structures. For the DC2 frames, the alternative capacity design rule to prevent formation of a soft storey plastic mechanism did not govern the design of the frames. On the other hand, the limitation of the interstorey drift to 2%, discussed in Section 2.5, constrained the dimensions of the main elements of certain structures, namely of frames 5S-TypeD and 3S-TypeB. The interested reader is forwarded to the work by De Visscher [2021] to obtain the full details.

4 Nonlinear static analysis

4.1 Pushover analysis

The previously designed frames are subjected to pushover analyses aiming at determining the respective target points for the limit states of 'damage limitation' DL, 'significant damage' SD, and 'near collapse' NC. Space constraints again allow only for a very brief description of the nonlinear models and analysis procedure. Complete information can be found in the work by De Visscher [2021]. The software SeismoStruct [15] is employed for the analyses, which takes into account material inelastic response through fibre-based frame modelling [16] and geometric nonlinear effects via a corotational approach [17], [18].

The mean material properties were defined as input for the uniaxial nonlinear material models. The concrete fibres follow the constitutive relations proposed by Mander et al. [19], which also provides the rules used to determine the confinement effects in the section core of beams and columns. The steel rebar fibres abide by the model proposed by Menegotto and Pinto [20]. The average steel yield strength, f_{ym}, indicated in Table 2, was obtained from a ratio between the average and characteristic strength f_{yk} derived from a large dataset of experimental results [21]. A distributed plasticity finite element formulation is employed for the frame elements, namely a force-based approach with five integration points (or integration sections). Several verifications to ensure dependability of results and control localisation of deformations at the local level were performed [22], [23]. The resulting capacity curves, obtained with an incremental first-mode pattern of loads, are shown in Figure 2.

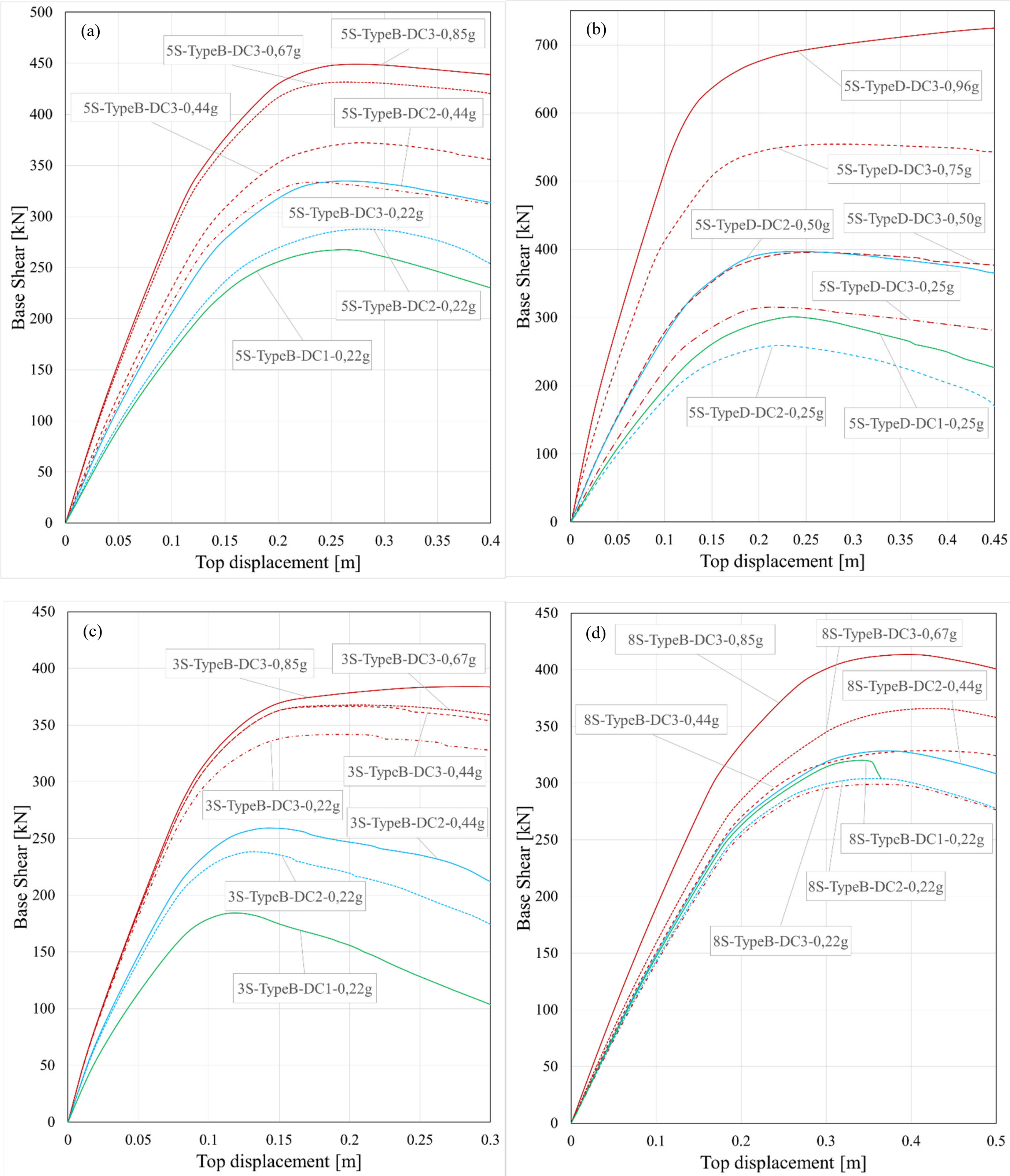

Figure 2. Pushover curves of the 28 RC frames: (a) 5S-TypeB, (b) 5S-TypeD, (c) 3S-TypeB, (d) 8S-TypeB.

The influence of the ductility classes in the structural response is clear. For identical design maximum spectral accelerations S_{α}, the DC3 frames show a more ductile behaviour, with longer plastic plateaus. In general, DC1 and DC2 structures depict steeper post-peak branches. DC3 structures also show a higher base shear strength (note the different scales of the abscissae and ordinate axes in the plots of Figure 2), which is instinctively less evident since the design base shear force is smaller than for the DC1 and DC2 frames (due to the larger behaviour factor). Once again, this can be explained by the strict capacity design rules imposed for the higher ductility class. Finally, for the same soil type (B), it is observed that the dispersion of the capacity curves reduces for increasing number of floors. In fact, the seismic design combination and corresponding criteria control the design of the stiffer low-rise structures with three storeys (3S-TypeB), whereas the gravity design combination tends to govern the design of the more flexible high-rise 8-storey frames (8S-TypeB).

4.2 Bilinearisation and target displacements

The previous capacity curves were converted through the participation factors Γ shown in Table 3 through Table 6 into equivalent SDoF force-deformation relations. Such capacity spectra were then bilinearised according to the indications of prEN 1998-1-1:2022 [1], as described in Section 2.3. It is noted that Point A in Figure 1 was determined for the first steel rebar yielding in the structure, and not for the first yield chord rotation. This was due to convenience in terms of the structural analysis program, but specific comparisons done for some frames showed the validity of this approximation. The resulting effective elastic periods T^* of the bilinearised capacity spectra are also reported in the tables.

The target displacements for the limit state SD were obtained with the N2 method, see Section 2.3. Additionally, in order to trace the evolution of deformations and the distribution of damage inside the structures, the target displacements corresponding to the limit states DL and NC were also computed. According to the new generation of EC8 [4], the elastic response spectra associated to the latter limit states can be obtained from the SD spectrum by application of a 'performance factor', to be defined by a relevant Authority or National Annex. For the consequence class CC2, the recommended values are 1.5 and 0.5 for NC and DL respectively.

The results of the nonlinear static procedures are shown in Table 3 through Table 6, wherein the displacements refer to the top storey in each frame (i.e. upon reconversion from d_{LS}^{*} to d_{LS}). The tables show that the displacements corresponding to attaining the limit states NC, SD and DL get closer as the seismic action parameter S_{α} decreases. Moreover, for structures designed with $S_{\alpha} = 0.25$g and $S_{\alpha} = 0.22$g (soil types D and B respectively), the three limit states are systematically located in the linear elastic region of the capacity curves, or at incipient levels of plasticity for NC. This can be seen by comparison with the plots in Figure 2, and can be easily understood since the seismic design combination does not control for these low levels of seismic action, rather the design of the frames is governed by the gravity design combination.

Table 3. Elastic properties, effective elastic period, and target displacements of frames 5S-TypeB for limit states DL, SD, and NC.

Frames 5S-TypeB						
Label	T_1 **[s]**	**Γ [-]**	T^* **[s]**	d_{DL} **[m]**	d_{SD} **[m]**	d_{NC} **[m]**
DC3-0.85g	1.14	1.42	1.36	0.104	0.209	0.313
DC3-0.67g	1.14	1.42	1.38	0.083	0.166	0.248
DC3-0.44g	1.29	1.32	1.58	0.058	0.117	0.176
DC3-0.22g	1.41	1.28	1.69	0.030	0.061	0.091
DC2-0.44g	1.37	1.32	1.67	0.062	0.124	0.185
DC2-0.22g	1.50	1.32	1.80	0.033	0.067	0.100
DC1-0.22g	1.50	1.23	1.92	0.033	0.066	0.099

Table 4. Elastic properties, effective elastic period, and target displacements of frames 5S-TypeD for limit states DL, SD, and NC.

Frames 5S-TypeD						
Label	T_1 **[s]**	**Γ [-]**	T^* **[s]**	d_{DL} **[m]**	d_{SD} **[m]**	d_{NC} **[m]**
DC3-0.96g	0.89	1.43	1.05	0.146	0.297	0.437
DC3-0.75g	0.90	1.34	1.16	0.118	0.237	0.355
DC3-0.50g	1.13	1.35	1.41	0.097	0.193	0.290
DC3-0.25g	1.40	1.28	1.68	0.054	0.109	0.163
DC2-0.50g	1.19	1.42	1.40	0.101	0.202	0.302
DC2-0.25g	1.48	1.28	1.80	0.058	0.117	0.175
DC1-0.25g	1.48	1.37	1.64	0.057	0.114	0.171

Table 5. Elastic properties, effective elastic period, and target displacements of frames 3S-TypeB for limit states DL, SD, and NC.

Frames 3S-TypeB						
Label	T_1 [s]	Γ [-]	T^* [s]	d_{DL} **[m]**	d_{SD} **[m]**	d_{NC} **[m]**
DC3-0.85g	0.82	1.19	1.05	0.068	0.135	0.203
DC3-0.67g	0.82	1.19	1.05	0.053	0.106	0.159
DC3-0.44g	0.82	1.19	1.05	0.035	0.070	0.106
DC3-0.22g	0.82	1.19	1.06	0.018	0.036	0.053
DC2-0.44g	0.93	1.19	1.21	0.040	0.081	0.121
DC2-0.22g	0.93	1.19	1.22	0.020	0.041	0.061
DC1-0.22g	1.11	1.19	1.35	0.023	0.045	0.068

Table 6. Elastic properties, effective elastic period, and target displacements of frames 8S-TypeB for limit states DL, SD, and NC.

Frames 8S-TypeB						
Label	T_1 [s]	Γ [-]	T^* [s]	d_{DL} [m]	d_{SD} **[m]**	d_{NC} **[m]**
DC3-0.85g	1.80	1.46	2.16	0.157	0.314	0.472
DC3-0.67g	2.07	1.45	2.34	0.123	0.245	0.368
DC3-0.44g	2.08	1.21	2.65	0.068	0.136	0.204
DC3-0.22g	2.16	1.21	2.74	0.034	0.068	0.102
DC2-0.44g	2.16	1.21	2.66	0.068	0.136	0.204
DC2-0.22g	2.16	1.21	2.72	0.034	0.068	0.102
DC1-0.22g	2.16	1.21	2.68	0.034	0.068	0.102

5 Displacement-based verification

5.1 Behaviour factor and its components

Based on the analyses performed in the previous section, it is possible to compute the actual reduction of the elastic forces for each frame and to calculate the three components of the behaviour factor q – namely q_S, q_R, and q_D – which were introduced in Section 2.2. The component q_S, accounting for over-design and overstrength, is not yet uniquely defined. Therefore, two alternative approaches are herein proposed. First, with reference to Figure 3, q_S is taken as the ratio F_y^*/F_{Ed}^* between the force corresponding to the yield displacement of the bilinear idealisation and the equivalent SDoF design force. In the second proposal, it is taken as $q_S = F_1^*/F_{Ed}^*$, where F_1^* is the force corresponding to the first yield chord rotation θ_y attained in one element in the structure (ε_y was herein taken as a proxy, as discussed in the previous section).

The component q_R is related with the structural redundancy, i.e. with the capacity of the structure to form several plastic hinges before reaching collapse. Two situations can occur: (i) the structural response is inelastic, i.e. $d_{SD}^* > d_y^*$. In this case, q_R is computed as the ratio between the force F_{SD}^* in the bilinear idealisation corresponding to the target displacement d_{SD}^*, and the force associated to the definition of q_S as discussed above. In other words, $q_R = F_{SD}^*/F_y^*$ for the first proposal and $q_R = F_{SD}^*/F_1^*$ for the second one (see Figure 3); (ii) the structure responds elastically, i.e. $d_{SD}^* < d_y^*$. In this case, q_R is computed using in the numerator the maximum force of the capacity spectrum, F_{max}^*, instead of F_{SD}^*, which provides a measure of the potential robustness of the structure. In other words, $q_R = F_{max}^*/F_y^*$ for the first proposal and $q_R = F_{max}^*/F_1^*$ for the second (Figure 3).

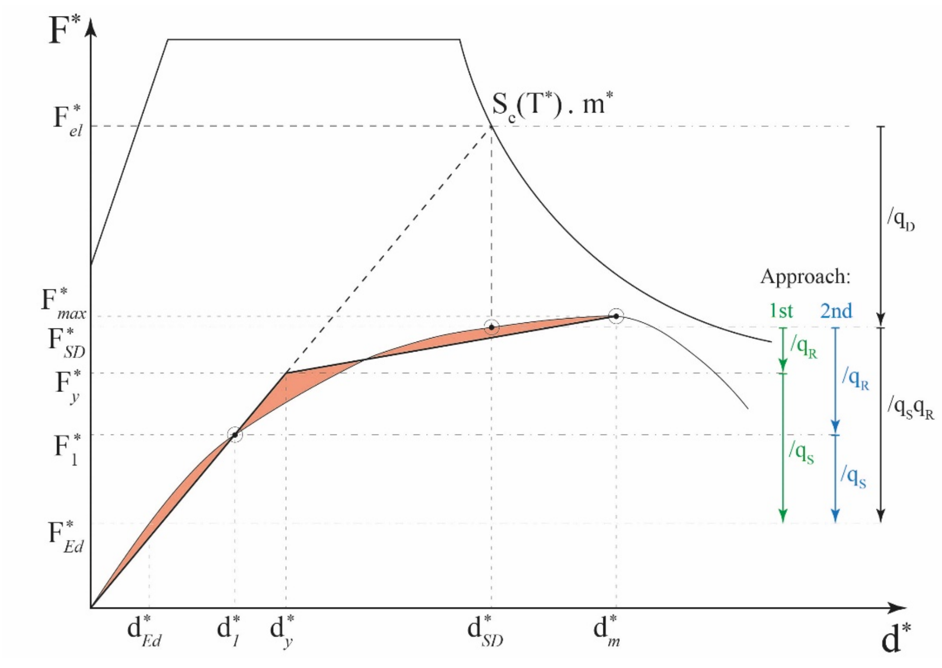

Figure 3. Illustration of the two approaches used to compute the components of the behaviour factor q.

Finally, the evaluation of the component q_D representing the energy dissipation capacity is only meaningful if the structure responds inelastically, i.e. if $d_{SD}^* > d_y^*$. In such case $q_D = F_{el}^*/F_{SD}^*$, where F_{el}^* corresponds to the intersection between the elastic response spectrum and the extension of the elastic branch of the bilinear idealisation (see Figure 3). Unlike for q_R, note that it is not possible to estimate the potential energy dissipation capacity of the structure if it responds elastically.

Table 7 presents a summary of the ratios used to compute the three components of the behaviour factor as described above, which depend on the approach adopted and the type of response (elastic or inelastic). The results of the application to all case studies can be found in Table 8. A first direct comparison between the behaviour factor used for design, q_{design}, and the one calculated after analysis, $q_{analysis}$, can be made for the frames where an inelastic response is observed, i.e. for $S_\alpha \geq 0.5$ g. It is apparent that in all such cases $q_{design} > q_{analysis}$, with an average of $q_{design} = 1.43 \times q_{analysis}$. The ratio $q_{design}/q_{analysis}$ gradually increases from the 3-storey to the 8-storey buildings. A thorough discussion to understand the difference between q_{design} and $q_{analysis}$ is given in Section 5.2. Table 8 also includes some information relative to those cases where an elastic structural response is obtained, namely: (i) cells in italics, which represent the potential maximum q_R according to the two approaches, as discussed above; (ii) a column $(q_S q_R)_{max}$ with the product of this potential maximum q_R and the corresponding q_S, and (iii) a column q_{min} with an estimated minimum behaviour factor. These points will be discussed in Section 5.2.

Considering again only the frames for which the response is inelastic, the overall average q_S for the two approaches is equal to 1.60, which is very close to the value of $q_S = 1.50$ assumed in the current and next EC8 generations. The two alternative approaches provide upper ($q_S = 1.89$) and lower ($q_S = 1.30$) bounds confirming that the first yield chord rotation θ_y should produce values of $q_S \approx 1.5$. Regarding the component q_R, the overall average of 1.29 is even closer to the prescribed code value (1.3). In other words, the main difference appears regarding the energy-dissipation component q_D, where the calculated average of 1.39 for DC3 is clearly lower than the prescribed value of 2.0 (although it should also be noted that for the particular case of frame 5S-TypeD-DC3-0.96g a close value of $q_D = 1.9$ was obtained). The reasons for this discrepancy will be further discussed in Section 5.2. It is also observed that the component q_D shows a tendency to reduce for lower values of spectral accelerations S_α. However, as it will be discussed in Sections 6.2 and 6.3, the values for this component q_D as obtained above are of no practical importance for engineering design. A graphical representation of the behaviour factor and its components, for DC3, is included in Figure 4.

Table 7. Summary of the ratios used to calculate the components of the behaviour factor q.

Approach	**q_S [-]**		**q_R [-]**		**q_D [-]**	
	Elastic	**Inelastic**	**Elastic**	**Inelastic**	**Elastic**	**Inelastic**
First	F_y^*/F_{Ed}^*		F_{max}^*/F_y^*	F_{SD}^*/F_y^*	–	F_{el}^*/F_{SD}^*
Second	F_1^*/F_{Ed}^*		F_{max}^*/F_1^*	F_{SD}^*/F_1^*		

Table 8. Behaviour factor and its components for the 28 RC frames: design *versus* calculated. Cells in italics indicate a potential maximum, corresponding to the cases where an elastic structural response is obtained.

Label		q_{design}	**1st Approach**		**2nd Approach**		q_D	$q_{analysis}$	$\frac{q_{design}}{q_{analysis}}$	$(q_S q_R)_{max}$	q_{min}
			q_S	q_R	q_S	q_R					
5S-TypeB	DC3-0.85g	3.9	1.7	1.1	1.2	1.6	1.4	2.6	1.50	-	-
	DC3-0.67g		1.9	1.0	1.3	1.5	1.2	2.3	1.70	-	-
	DC3-0.44g		3.3	*1.1*	2.3	*1.6*	-	-	-	*3.7*	3.3
	DC3-0.22g		6.5	*1.1*	4.8	*1.5*	-	-	-	*7.2*	6.5
	DC2-0.44g	2.5	2.0	*1.1*	1.5	*1.5*	-	-	-	*2.2*	2.0
	DC2-0.22g		3.9	*1.1*	2.8	*1.5*	-	-	-	*4.2*	3.9
	DC1-0.22g	1.5	2.0	*1.1*	1.7	*1.4*	-	-	-	*2.3*	2.0
5S-TypeD	DC3-0.96g	3.9	1.5	1.1	1.1	1.5	1.9	3.1	1.26	-	-
	DC3-0.75g		1.6	1.1	1.1	1.7	1.7	2.9	1.34	-	-
	DC3-0.50g		2.1	1.0	1.4	1.6	1.3	2.9	1.34	-	-
	DC3-0.25g		3.6	*1.1*	2.7	*1.5*	-	-	-	*4.0*	3.6
	DC2-0.50g	2.5	1.5	1.0	1.1	1.5	1.3	2.0	1.25	-	-
	DC2-0.25g		2.2	*1.1*	1.6	*1.5*	-	-	-	*2.4*	2.2
	DC1-0.25g	1.5	1.6	*1.1*	1.2	*1.6*	-	-	-	*1.8*	1.6
3S-TypeB	DC3-0.85g	3.9	2.3	1.0	1.5	1.5	1.4	3.2	1.22	-	-
	DC3-0.67g		2.8	1.0	1.9	1.5	1.1	3.2	1.22	-	-
	DC3-0.44g		4.3	*1.1*	2.9	*1.6*	-	-	-	*4.7*	4.3
	DC3-0.22g		7.9	*1.1*	5.2	*1.6*	-	-	-	*8.5*	7.9
	DC2-0.44g	2.5	2.3	*1.1*	1.6	*1.5*	-	-	-	*2.5*	2.3
	DC2-0.22g		4.2	*1.1*	2.9	*1.5*	-	-	-	*4.5*	4.2
	DC1-0.22g	1.5	2.1	*1.0*	1.4	*1.5*	-	-	-	*2.1*	2.1
8S-TypeB	DC3-0.85g	3.9	1.6	1.1	1.1	1.5	1.4	2.4	1.63	-	-
	DC3-0.67g		1.9	1.0	1.3	1.4	1.1	2.1	1.86	-	-
	DC3-0.44g		2.6	*1.1*	1.9	*1.5*	-	-	-	*2.9*	2.6
	DC3-0.22g		5.0	*1.1*	3.8	*1.4*	-	-	-	*5.4*	5.0
	DC2-0.44g	2.5	2.0	*1.1*	1.5	*1.5*	-	-	-	*2.2*	2.0
	DC2-0.22g		3.9	*1.1*	3.0	*1.4*	-	-	-	*4.2*	3.9
	DC1-0.22g	1.5	2.3	*1.1*	3.0	*1.5*	-	-	-	*3.5*	2.3

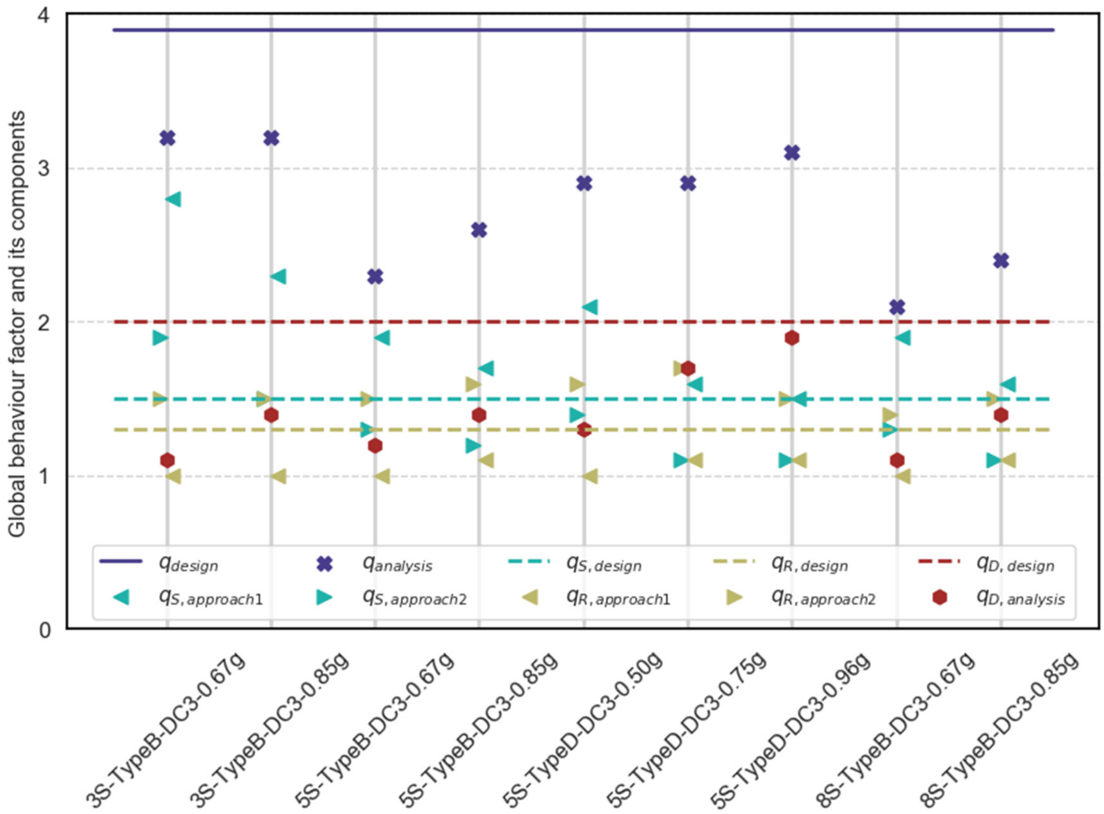

Figure 4. Behaviour factor q and its components, for ductility class DC3: comparison between current design specifications (subscript "design") and the real exploited values as calculated from analysis (subscripts "analysis" and "approach").

5.2 Discussion on design and calculated behaviour factors

In engineering practice the initial design of a structure is, and will remain, a force-based design relying on linear elastic analyses. Many specifications in EC8, either in its current or future generation, are directed to guarantee that the default upper-bound values of the behaviour factor q_{design}, prescribed in the code, can be attained. They include, among others, "strong column – weak beam" requirements and other capacity design rules for the beams, columns, and beam-column joints. Note that, at this design stage, the engineer has already pre-designed the frame member geometry, which is used to compute the seismic shear demand from the elastic response spectrum. The latter is usually determined through a fundamental period computed from a numerical model incorporating estimated effective elastic stiffnesses of the structural members.

However, several aspects may limit the exploitation of the upper bound values for q_{design} given in EC8. They include drift limitations imposed by the code, as discussed in Section 2.5, or simply the fact that for lower levels of seismic action the gravity design combination governs, instead of the seismic design combination. One of the consequences is that such structures are required to be stiffer and stronger than what would be needed from seismic design alone, and usually their seismic response remains below the yield point. It is therefore neither simple nor direct to determine the extent to which the regulations associated to assure a certain

q_{design} impact or control the actual design of the frames. To put it in another way, the interaction between multiple requirements – beyond the rules explicitly aiming at guaranteeing a certain ductility capacity and energy dissipation – is likely to change significantly the repartition of the components q_S, q_R, and q_D of the real value of the exploited behaviour factor, $q_{analysis}$. A quick inspection of the case studies for which an elastic response was obtained illustrates the previous comment. For these structures, as mentioned in Section 5.1, it is not possible to determine q_D, as the computation of this component requires an inelastic response (see Figure 3). The same rationale applies to the component q_R, for which only a potential maximum value can be determined as listed in Table 8 (cells in italic) following the definition in Table 7. In order to bypass the two alternative approaches to compute q_S and q_R, Table 8 includes a column $(q_S q_R)_{max}$ with the product of the conceivable maximum q_R and the corresponding q_S. The only component of the behaviour factor that can be computed is q_S, in its form F_y^*/F_{Ed}^*, which corresponds to a minimum implicit value of the real behaviour factor that can be ascribed to each structure. This value is listed in the column q_{min} of Table 8. It can be noted that this value is, for most case studies, only marginally smaller than $(q_S q_R)_{max}$. More importantly, it is observed that for most structures, q_{min} is close to or even larger than q_{design}, i.e. the default upper-bound values given in EC8. Additionally, this minimum behaviour factor does not reduce with respect to the behaviour factor corresponding to those cases governed by the seismic design combination (i.e. column $q_{analysis}$ in Table 8), which result from the product of the three components q_S, q_D, and q_R.

The combination of all design provisions usually lead the design engineer to adjust the member cross-section geometries and the reinforcement detailing, with respect to the initial pre-design phase. If such changes are significant, it may be justified to recompute the design base shear from the revised structural dynamic properties, which highlights the potential iterative character of the design procedure.

Be it for the computation of the shear demand with the initial pre-designed sections, or with the revised ones, one factor significantly and consistently contributes to keep the gap between q_{design} and the calculated $q_{analysis}$ shown in Table 8 and in Figure 4 for the cases where an inelastic response is attained: the elastic stiffness assigned to the numerical model. In fact, the common use of one-half of the corresponding stiffness of the uncracked members, as permitted by the code, provides stiffer structures with respect to the more accurate bilinearisation of the pushover curves, as illustrated in Table 3 through Table 6 by comparing periods T_1 and T^*. Two immediate consequences arise. Firstly, the verification of the codified drift limits may become non-conservative. Secondly, the elastic design force $F_{el,design}^*$ will in general (for $T^* > T_C$) become larger than F_{el}^*, and hence so does q_{design} with respect to $q_{analysis}$. This also explains why the main difference, in terms of the behaviour factor components, shows up regarding the energy-dissipation component q_D, computed as F_{el}^*/F_{SD}^* (see Figure 3).

The above discussion suggests the need to improve the estimate of the effective elastic flexural member stiffnesses for design. More complete and straightforward engineering guidance would be welcome, as given in other international codes (Section 2.5).

5.3 Global and local verification coefficients

In a displacement-based approach, the global and local verifications are outlined according to expressions (3) and (4). In the present section, such equations are solved for $\alpha_{SD,d}$ and $\alpha_{SD,\delta}$. As discussed, for RC frame structures, δ corresponds to the chord rotation θ, and the notation $\alpha_{SD,\theta}$ is therefore adopted. Regarding the computation of $\alpha_{SD,d}$, the following comments are important: (i) the displacement d_u^* is obtained from the structural displacement d_u corresponding to the attainment of the first ultimate chord rotation θ_u in one element in the structure; θ_u was calculated according to the expressions defined in Part 3 of the current Eurocode 8 [24], which are computed automatically by the structural analysis software [15], assuming mean material properties and no safety factors for consistency with the analysis and verification assumptions. Actually, the current Part 3 of EC8 and the analysis software also consider the attainment of the shear capacity of an element as the ultimate displacement, but this was not reached for the present case studies; (ii) the yield displacement d_y^* was computed through the bilinearisation of the capacity spectra; (iii) the partial factor $\gamma_{Rd,SD,d}$ was taken as equal to unity; (iv) d_{SD}^* was computed as discussed in Section 4.2.

With respect to the calculation of $\alpha_{SD,\theta}$, it was derived assuming: (i) a chord rotation at yielding θ_y and a plastic part of the chord rotation θ_u^{pl} evaluated according to prEN 1998-1-1:2022 [1]; (ii) a partial factor $\gamma_{Rd,SD,\theta} = \gamma_{Rd,k} \cdot s_\gamma = 1.575$, corresponding to $\gamma_{Rd,k} = 1.5$ [1] and a shape factor for rectangular sections $s_\gamma = 1.05$ [4]; (iii) $\delta_{SD} = \theta_{SD}$ corresponding to the chord rotation, for each extremity of each element, attained at a top displacement d_{SD}.

Computations of $\alpha_{SD,\theta}$ were done for both extremities of all the columns and beams in each frame. The complete results can be found in the work by De Visscher [2021]. The largest values, obtained among all the columns, $\alpha_{SD,\theta,c}$, and all the beams, $\alpha_{SD,\theta,b}$, are shown in Table 9 through Table 12. These tables also show the results obtained for the global verification, $\alpha_{SD,d}$. They also include the results computed for the other ultimate limit state, NC, obtained assuming analogous considerations as discussed in the previous paragraphs for the limit state SD. Finally, Figure 5 includes a graphical representation for the DC3 frames.

Table 9. Global and local (index c: columns; index b: beams) verification coefficients for the frames 5S-TypeB.

Frames 5S-TypeB						
Label	$\alpha_{SD,d}$	$\alpha_{SD,\theta,b}$	$\alpha_{SD,\theta,c}$	$\alpha_{NC,d}$	$\alpha_{NC,\theta,b}$	$\alpha_{NC,\theta,c}$
DC3-0.85g	0.13	0.29	0.14	0.32	0.64	0.48
DC3-0.67g	0.05	0.25	0.05	0.20	0.39	0.24
DC3-0.44g	—	0.24	—	0.04	0.37	0.02
DC3-0.22g	—	0.04	—	—	0.13	—
DC2-0.44g	—	0.29	—	0.21	0.41	0.05
DC2-0.22g	—	0.09	—	—	0.25	—
DC1-0.22g	—	0.10	—	—	0.21	—

Table 10. Global and local (index *c*: columns; index *b*: beams) verification coefficients for the frames 5S-TypeD.

Frames 5S-TypeD						
Label	$\alpha_{SD,d}$	$\alpha_{SD,\theta,b}$	$\alpha_{SD,\theta,c}$	$\alpha_{NC,d}$	$\alpha_{NC,\theta,b}$	$\alpha_{NC,\theta,c}$
DC3-0.96g	0.25	0.55	0.43	0.48	0.95	0.84
DC3-0.75g	0.17	0.38	0.22	0.36	0.76	0.61
DC3-0.50g	0.08	0.38	0.05	0.24	0.58	0.26
DC3-0.25g	—	0.23	—	0.06	0.36	0.08
DC2-0.50g	0.09	0.19	0.08	0.27	0.45	0.34
DC2-0.25g	—	0.28	—	0.08	0.44	0.07
DC1-0.25g	—	0.25	—	0.01	0.37	—

Table 11. Global and local (index c: columns; index b: beams) verification coefficients for the frames 3S-TypeB.

Frames 3S-TypeB						
Label	$\alpha_{SD,d}$	$\alpha_{SD,\theta,b}$	$\alpha_{SD,\theta,c}$	$\alpha_{NC,d}$	$\alpha_{NC,\theta,b}$	$\alpha_{NC,\theta,c}$
DC3-0.85g	0.23	0.48	0.24	0.56	0.79	0.62
DC3-0.67g	0.03	0.37	0.12	0.19	0.59	0.38
DC3-0.44g	—	0.23	—	0.03	0.35	0.10
DC3-0.22g	—	0.06	—	—	0.11	—
DC2-0.44g	—	0.31	—	0.32	0.55	0.24
DC2-0.22g	—	0.09	—	—	0.16	—
DC1-0.22g	—	0.14	—	—	0.34	—

Table 12. Global and local (index *c*: columns; index *b*: beams) verification coefficients for the frames 8S-TypeB.

Frames 8S-TypeB						
Label	$\alpha_{SD,d}$	$\alpha_{SD,\theta,b}$	$\alpha_{SD,\theta,c}$	$\alpha_{NC,d}$	$\alpha_{NC,\theta,b}$	$\alpha_{NC,\theta,c}$
DC3-0.85g	0.14	0.34	0.02	0.34	0.69	0.29
DC3-0.67g	0.10	0.27	—	0.52	0.46	0.06
DC3-0.44g	—	0.13	—	—	0.25	—
DC3-0.22g	—	0.00	—	—	0.08	—
DC2-0.44g	—	0.14	—	—	0.26	—
DC2-0.22g	—	—	—	—	0.08	—
DC1-0.22g	—	—	—	—	0.07	—

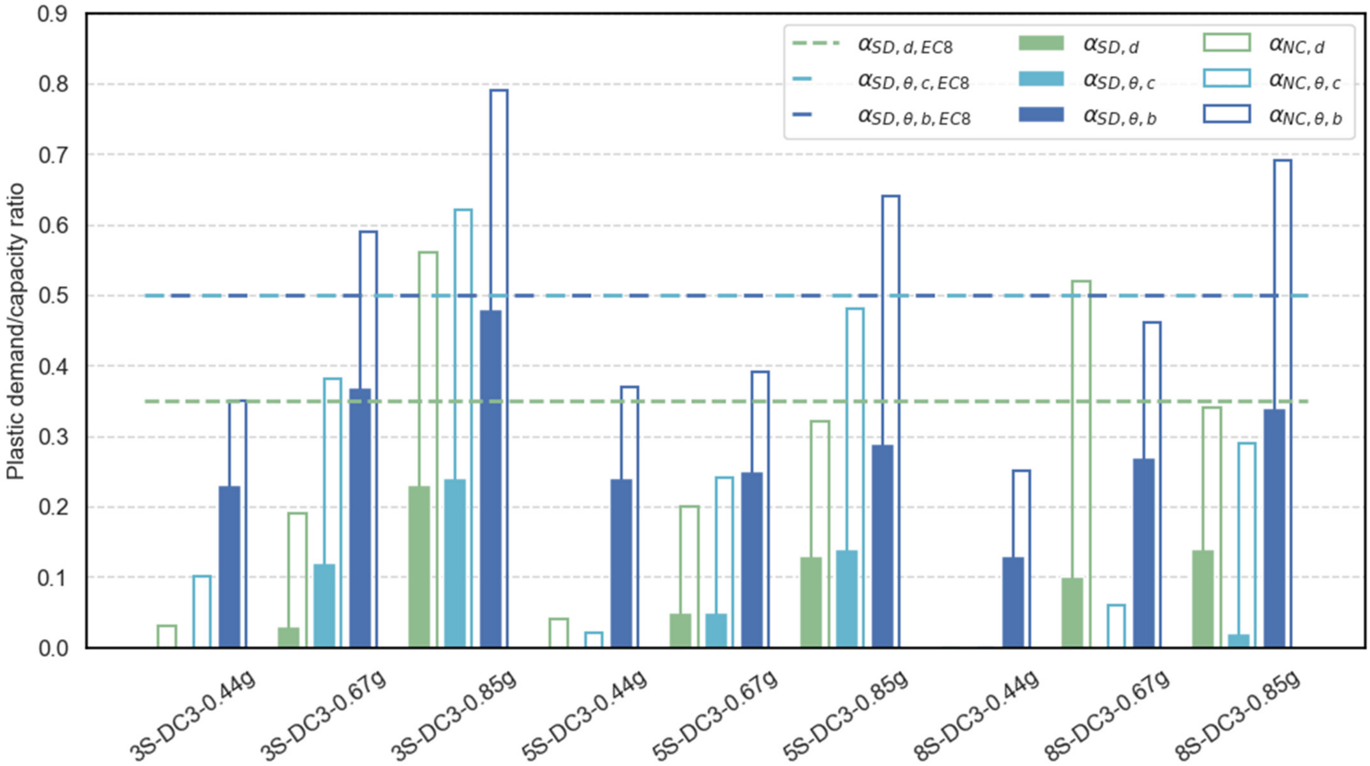

Figure 5. Plastic demand/capacity ratios for the frames designed for ductility class DC3, soil Type B; both global and local (columns and beams) verifications are depicted for the limit states of significant damage (SD) and near collapse (NC).

The tables show a maximum coefficient $\alpha_{SD,d}$ of 0.25 (for soil type D), and for most frames such coefficient is considerably smaller than the reference value of 0.35 defined in prEN 1998-1-1:2022 [1]. This can be partly explained by the unitary value assumed for the partial factor $\gamma_{Rd,SD.d}$. It is also observed that with the exception of frames 5S-TypeD-DC3-0.96g and 3S-TypeB-DC3-0.85g, no structure reaches the local deformation limit of $\alpha_{SD,\theta} = 0.5$ (refer to Section 2.4); the frame members present in general a large reserve of capacity, shown by low values of $\alpha_{SD,\theta}$. Moreover, it is observed that $\alpha_{SD,\theta,b} > \alpha_{SD,\theta,c}$, which highlights the desired effects of capacity design rules. It is therefore expected that energy dissipation takes place at the ends of the beams and not in the columns, extending over the height of the structure and therefore promoting a global beam-sway mechanism. This can be confirmed in Figure 6, which shows the locations where steel rebars have reached a value of strain $\varepsilon > \varepsilon_y$.

Unreported results also show that, for the damage limitation limit state, the frames incur on negligible plastification. It occurs in very few locations in the 3-storey frames, and even less in the 5-storey structures. In between the limit states of significant damage and near collapse, the progression of plastic hinge formation continues to concentrate at the extremities of the beams and base of the columns, i.e. according to the desired failure mechanism.

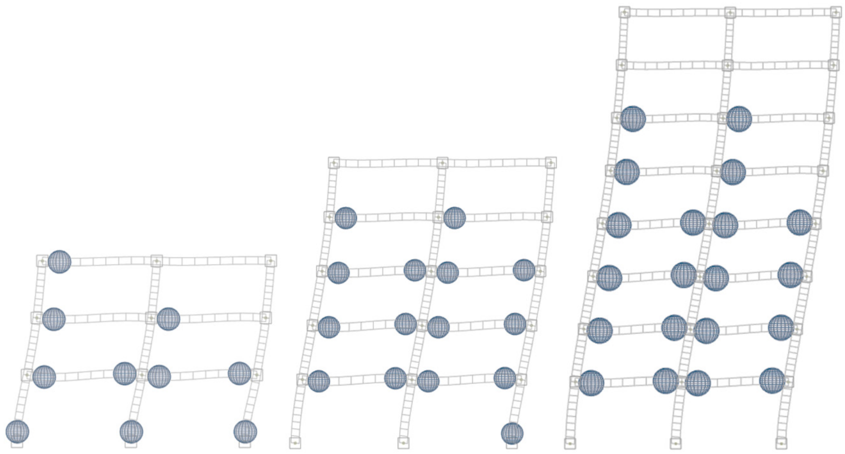

Figure 6. Deformed shape of frames 3S-TypeB-DC3-0.85g, 5S-TypeB-DC3-0.85g, and 8S-TypeB-DC3-0.85g at the limit state of significant damage, highlighting the locations where yielding is attained.

6 Discussion and calibration

6.1 Influence of design parameters

An analysis of the results obtained in Section 5.2 allows extracting conclusions regarding the influence of some design parameters. Firstly, for the same seismic action parameter S_α and soil type, it can be observed that the exploitation of the available plastic deformation capacity is higher for the lower ductility classes. This can be confirmed in particular by comparing the values of $\alpha_{SD,\theta,b}$ in Table 9 through Table 12 for the various frames designed in soil B for S_α = 0.22g with ductility classes DC1, DC2, and DC3, or S_α = 0.44g with ductility classes DC2 and DC3. Although a lower ductility class implies a lower reduction of the elastic to the design base shear, and therefore larger seismic action effects, the capacity design provisions of EC8 for the higher ductility classes endow the structures with an overall higher base shear capacity and a larger effective elastic stiffness (see Figure 2). In turn, this promotes target displacements that are generally higher for DC1 and DC2, when compared with DC3 (see Table 3 through Table 6). Moreover, the plastic deformation capacity is lower for ductility class DC1 with respect to DC2, and DC2 with respect to DC3; this smaller plastic deformation capacity for the lower ductility classes facilitates attaining higher values of $\alpha_{SD,\theta,b}$.

Secondly, the tables of the previous section also indicate a clear influence of the level of seismic action parameter S_α considered for design. Thirdly, the comparison of the results obtained for the frames 5S-TypeB and 5S-TypeD also show an indisputable influence of the soil type, which goes beyond the level of spectral acceleration S_α. Note, for instance, that the value of $\alpha_{\mathrm{SD},\theta,\mathrm{b}}$ attained for the frame 5S-TypeD-DC3-0.25g is sensibly similar to the value of $\alpha_{\mathrm{SD},\theta,\mathrm{b}}$ attained for the frame 5S-TypeB-DC3-0.67g. The soil type can strongly influence the combination governing the structural design (seismic versus gravity).

Finally, the results also reveal that the number of floors clearly affect the inelastic demands. For the 3-storey frames, the local plastic deformations are significant at the base of the columns and particularly at the first floor beams – steeply reducing for the upper storeys, whereas the 8-storey frames show smaller but more evenly distributed plastic beam deformations over the whole structure, together with essentially elastic column response.

6.2 Simplified approach for estimating an harmonised behaviour factor

The method proposed in this section aims at estimating behaviour factors, $q_{estimated}$, coherent with the local verification limits of the displacement-based approach. It is applied to each of the case-study frames and consists of the following steps: (i) identification of the top displacement $d_{\alpha_\theta=0.5}$ at which a maximum value of $\alpha_{SD,\theta} = 0.5$ is attained in one frame member extremity; such values, shown in Table 13, can be positioned on the pushover curves of Figure 2; (ii) inversion of the N2 method (keeping the same spectral shape of each soil type) to determine $S_{\alpha,\alpha_\theta=0.5}$ for which the target displacement corresponds to $d_{\alpha\theta=0.5}$; (iii) determination of the associated behaviour factor $q_{estimated}$, as discussed in Section 5.1. Table 13 shows these results.

As expected, it is observed that the value of $S_{\alpha,\alpha_\theta=0.5}$ does not increase significantly for those cases where $\alpha_{SD,\theta}$ was already very close or larger than 0.5, namely for the frames 5S-TypeD-DC3-0.96g (where $S_{\alpha,\alpha_\theta=0.5} = S_\alpha = 9.6$ m/s^2) and 3S-TypeB-DC3-0.85g (where it increases from $S_\alpha = 8.5$ m/s^2 to $S_{\alpha,\alpha_\theta=0.5} = 9.1$ m/s^2). On the other hand, for lower seismic intensities, the increase can be quite significant, as shown by the ratio $S_{\alpha,\alpha_\theta=0.5}/S_\alpha$ in the next to last column of Table 13. For many such cases, the design was controlled by the gravity design combination and it is therefore meaningless to derive $q_{estimated}$ based on the previous approach. Moreover, the value $S_{\alpha,\alpha_\theta=0.5}$ for all DC1 frames is above the maximum design pseudo-acceleration $S_{\alpha=DC1} = 3\ m/s^2$, which would therefore require a design according to DC2 or DC3. In other words, the method described above is not applicable in general and can at best provide first rough estimates of harmonised behaviour factors for seismic intensities S_α larger than around 0.4-0.5g.

Table 13. Original design versus estimated behaviour factor from analysis leading to $\alpha_{SD,\theta} = 0.5$, using simplified approach.

Label		q_{design}	S_α [m/s^2]	$d_{\alpha_\theta=0.5}$ [m]	$S_{\alpha,\alpha_\theta=0.5}$ [m/s^2]	$\frac{S_{\alpha,\alpha_\theta=0.5}}{S_\alpha}$	$q_{estimated}$
5S-TypeB	DC3-0.85g	3.9	8.5	0.279	11.4	1.3	3.5
	DC3-0.67g		6.7	0.277	11.2	1.7	3.9
	DC3-0.44g		4.4	0.233	8.8	2.0	5.1
	DC3-0.22g		2.2	0.240	8.8	4.0	10.9
	DC2-0.44g	2.5	4.4	0.225	8.1	1.8	3.0
	DC2-0.22g		2.2	0.210	7.0	3.2	5.3
	DC1-0.22g	1.5	2.2	0.205	6.9	3.1	3.0
5S-TypeD	DC3-0.96g	3.9	9.6	0.297	9.6	1.0	3.1
	DC3-0.75g		7.5	0.282	9.0	1.2	3.5
	DC3-0.50g		5.0	0.256	6.6	1.3	3.9
	DC3-0.25g		2.5	0.216	5.0	2.0	5.5
	DC2-0.50g	2.5	5.0	0.320	8.0	1.6	3.2
	DC2-0.25g		2.5	0.192	4.1	1.6	2.9
	DC1-0.25g	1.5	2.5	0.224	4.9	2.0	2.2
3S-TypeB	DC3-0.85g	3.9	8.5	0.144	9.1	1.1	3.4
	DC3-0.67g		6.7	0.140	8.8	1.3	4.1
	DC3-0.44g		4.4	0.140	8.8	2.0	6.2
	DC3-0.22g		2.2	0.135	8.4	3.8	12.5
	DC2-0.44g	2.5	4.4	0.114	6.2	1.4	2.9
	DC2-0.22g		2.2	0.114	6.2	2.8	5.8
	DC1-0.22g	1.5	2.2	0.110	5.5	2.5	2.8
8S-TypeB	DC3-0.85g	3.9	8.5	0.390	10.6	1.2	2.9
	DC3-0.67g		6.7	0.390	10.6	1.6	3.4
	DC3-0.44g		4.4	0.343	11.2	2.5	4.2
	DC3-0.22g		2.2	0.329	10.8	4.9	7.7
	DC2-0.44g	2.5	4.4	0.318	11.2	2.5	3.3
	DC2-0.22g		2.2	0.306	10.0	4.5	5.6
	DC1-0.22g	1.5	2.2	0.318	10.4	4.7	3.7

However, the biggest difficulty of the previous approach is arguably the fact that $q_{estimated}$ is based on bilinearised curves obtained from nonlinear analyses, whereas the structural force-based design relied on spectral shear demands computed with linear elastic analyses (and cracked sectional inertias) to which q_{design} was applied. As an example, it can be readily seen from Table 13 that for frame 5S-TypeD-DC3-0.96g the desired design behaviour factor is indeed the one initially prescribed ($q_{design} = 3.9$), and not the one computed from analysis ($q_{estimated} = 3.1$). Evidently, it is q_{design} that should be calibrated for harmonisation between FB and DB approaches (with particular focus on its component q_D), since it is the one used for design. However, the above observation further reinforces the need – as a preliminary step to any harmonisation procedure, and as discussed in Section 5.2, to improve the estimates of the effective elastic member stiffnesses.

6.3 Proposed harmonisation procedure for design behaviour factor

In order to overcome the limitations of the previous method, the present section suggests a procedure for the harmonisation of force-based and displacement-based design approaches in the context of the next generation of Eurocode 8. It is again underlined that, prior and complementary to such method, an improvement of simple guidance for the effective elastic stiffness should be performed, in order to reduce the global frame stiffness overestimation provided by assuming one-half of the uncracked member stiffnesses. The proposed harmonisation procedure requires an iterative procedure to determine the design behaviour factor q_{design} producing the target plastic deformation at the local level, expressed by a coefficient $\alpha_{SD,\theta} = 0.5$. Such behaviour factor (and its components) should be recommended in the code for FB design. Currently, as discussed in Section 2.2, q_{design} depends only on the structural type and ductility class. However, taking into account the conclusions in Section 6.1, it is herein proposed that it should depend additionally on: (i) the seismic action and soil type, which jointly determine the design spectrum, in turn defined by combinations of the spectral accelerations S_α and S_β, and (ii) the number of storeys. For the sake of ease of application in engineering design practice, it is suggested that S_α and S_β are grouped into significant ranges, and that the moment resisting frames are also gathered in a few ranges of storeys. The proposed procedure starts with the definition of an extensive set of RC frames covering the representative ranges of the seismic action spectral parameters S_α and S_β, on the one hand, and number of storeys, on the other. The following steps should then be carried out for each RC frame, in each of the three ductility classes (for DC1 only up to $S_{\alpha=DC1} = 3\ m/s^2$):

1. Design the RC frame considering the gravity and seismic design combinations with a behaviour factor q_{design} (if it is the first iteration, the currently proposed upper-bound value can be used to start the iterative process). Build the nonlinear model, perform pushover analysis, bilinearise the capacity spectrum, and determine the target displacement (see Section 4). Then: (i) compute the behaviour factor $q_{analysis}$ and its components q_S and q_R (see Section 5.1); (ii) determine the component q_D as $q_D = q_{analysis}/(q_S q_R)$; (iii) calculate the coefficient $\alpha_{SD,d}$ and the maximum $\alpha_{SD,\theta}$ among the frame member extremities (see Section 5.2).
2. If the global seismic response is elastic, i.e. $d^*_{SD} < d^*_y$, the structural design is likely controlled by the gravity design combination and $\alpha_{SD,\theta}$ is smaller than 0.5. In this case, the implicit minimum behaviour factor is F^*_y/F^*_{Ed}, and one can also determine $(q_S q_R)_{max}$, i.e. the product of the component q_S and the measure of the potential robustness of the structure $q_{R,max}$ (see Section 5.1).

3. If the global seismic response is inelastic, i.e. $d^*_{SD} > d^*_y$, and $\alpha_{SD,\theta} < 0.5$, repeat step 1 with a larger value for q_{design}.
4. If the global seismic response is inelastic, i.e. $d^*_{SD} > d^*_y$, and $\alpha_{SD,\theta} > 0.5$, repeat step 1 with a smaller value for q_{design}.
5. If the global seismic response is inelastic, i.e. $d^*_{SD} > d^*_y$, and $\alpha_{SD,\theta} \approx 0.5$, save the values of q_{design}, its components (q_S, q_R, and q_D), as well as $\alpha_{SD,d}$.
6. Perform a regression analysis to determine a relation between the saved values of the behaviour factors (q_{design}, q_S, q_R, q_D) and the predictors (namely the ductility class, the ranges of S_α and S_β, and the number of storeys). The preliminary results of Section 5.1 indicate that the main dependent variable to be calibrated is the energy-dissipation component q_D; on the other hand, the components q_S and q_R are expected to not differ much from the values currently proposed for the next generation, i.e. q_S = 1.5 and q_R =1.3. It is also suggested to determine the range of the predictors for which an elastic response is expected, with indication of the product $(q_S q_R)_{max}$.
7. Perform a new regression analysis to determine a relation between $\alpha_{SD,d}$ and the predictors. A new set of recommended values for $\alpha_{SD,d}$ can hence be proposed for the design code, replacing the current fixed value of 0.35. As it refers to the global verification, the new proposals for $\alpha_{SD,d}$ should include a certain degree of conservatism.

The above harmonisation procedure is cast within the context of specific application to RC moment resisting frames regular in plan and in elevation, but it could be directly extended to frames irregular in plan and/or elevation, or to other structural types, including wall structures and equivalent dual structures. This will be the subject of future studies.

7 Conclusions

The next generation of the Eurocode 8 will provide the possibility to perform global and local displacement-based verifications using nonlinear seismic analysis. The present work studies the consistency between the latter verifications and the classical force-based design approach employing a behaviour factor, which is given as the product of three components: q_S (representing over-design and overstrength), q_R (representing redundancy), and q_D (representing energy dissipation capacity). To do so, 28 reinforced concrete moment resisting frames, regular in plan and in elevation, with three, five, and eight stories were designed according to the rules of the three new ductility classes (DC1, DC2, and DC3), for different levels of seismic action and two distinct soil types. These structures were then subjected to pushover analyses using a nonlinear model, followed by a new codified bilinearisation procedure and the determination of the corresponding target displacements with the N2 method. The limit states of damage limitation, significant damage, and near collapse were considered. The influence of the ductility classes in the structural response was clear, and as expected the DC3 structures showed a more ductile behaviour, whereas the DC1 and DC2 RC frames depicted steeper post-peak softening branches. However, the DC3 structures – which were designed with larger behaviour factors – also showed a higher base shear strength, an apparent contradiction that can be explained by the imposed stricter capacity design rules of this class. Moreover, for the frames designed for lower seismic action, the limit states were systematically located in the linear elastic region of the capacity curves, or at incipient levels of plasticity for near collapse, showing the prevalence of the gravity design combination with respect to the seismic design combination.

This investigation proposed and applied two alternative methods – based on the bilinear representation of the capacity spectrum – to determine the components q_S and q_R of the behaviour factor. The obtained values aligned well with the suggested values in the new version of the EC8, respectively 1.5 and 1.3. The presented method also allows computing the global behaviour factor, $q_{analysis}$, which is seen to be typically smaller than the behaviour factor used for design, q_{design}. The main reason for this discrepancy amounts to the fact that the bilinear representation of the frame response has an elastic period larger than the fundamental period of the elastic cracked model assumed for design, suggesting the need to revise the currently proposed method to estimate the effective elastic flexural member stiffnesses in design. It was also shown that the current values of q_{design} provide too conservative estimates (i.e. lower than target) of the global and local coefficients $\alpha_{SD,d}$ and $\alpha_{SD,\theta}$, which are at the core of the verifications in the displacement-based approach. A procedure to harmonise the latter with the force-based approach is therefore proposed and outlined in this research, which should be applied after guidance improvement on simple methods to better estimate the effective elastic stiffness. It aims at deriving new values for q_{design}, with particular focus on its component q_D, such that a newly designed structure attains the desired local demand in terms of exploitation of the available plastic deformation capacity for the limit state of significant damage. This procedure builds on new additional design parameters that were shown to govern the response, alongside with the structural typology and the ductility level, namely the seismic action and shape of the design response spectrum, as well as the number of storeys. It is also suggested that $\alpha_{SD,d}$ be calibrated for consistency between the local and global level verifications.

Declaration of Competing Interest

The authors declare that they have no known competing financial interests or personal relationships that could have appeared to influence the work reported in this paper.

Acknowledgments

The authors wish to acknowledge the work performed by Mr. Hélder Maranhão and Dr. José Melo under the supervision of Prof. Humberto Varum, which is at the origin of the case studies considered in this work. The comments by Prof. André Plumier regarding specific development phases of this work are also highly appreciated.

References

[1] CEN (European Committee for Standardization), *Eurocode 8 — Design of structures for earthquake resistance — Part 1-1: General rules and seismic action (Working Draft)*. 2022.

[2] CEN (European Committee for Standardization), *Eurocode 8 — Design of structures for earthquake resistance - Part 1: General rules, seismic actions and rules for buildings*. 2004.

[3] M. J. N. Priestley, G. M. Calvi, and M. J. Kowalsky, *Displacement-based Seismic Design of Structures*. IUSS Press - Istituto Universitario di Studi Superiori di Pavia, 2007.

[4] CEN (European Committee for Standardization), *Eurocode 8 — Design of structures for earthquake resistance — Part 1-2: Buildings (Working Draft)*. 2022.

[5] American Society of Civil Engineers, *ASCE standard, ASCE/SEI, 41-17, seismic evaluation and retrofit of existing buildings*, no. June. 2017.

[6] Applied Technology Council, "ATC 40: Seismic evaluation and retrofit of concrete buildings," 1996.

[7] P. Fajfar and P. Gaspersic, "The N2 method for the seismic analysis of RC buildings," *Earthq. Eng. Struct. Dyn.*, vol. 25, no. 1, pp. 31–46, 1996.

[8] P. Fajfar, "A Nonlinear Analysis Method for Performance Based Seismic Design," *Earthq. Spectra*, vol. 16, no. 3, pp. 573–592, 2000.

[9] N. M. Newmark and W. J. Hall, "Earthquake spectra and design," *Eng. Monogr. Earthq. Criteria*, 1982.

[10] T. Vidic, P. Fajfar, and M. Fischinger, "Consistent inelastic design spectra: strength and displacement," *Earthq. Eng. Struct. Dyn.*, vol. 23, no. 5, pp. 507–521, 1994.

[11] J.-M. Wong, A. Sommer, K. Briggs, and C. Ergin, "Effective Stiffness for Modling Reinforced Concrete Structures - A Literature Review," *Struct. Mag.*, pp. 18–21, 2017.

[12] CEN (European Committee for Standardization), *Eurocode 2: Design of concrete structures - Part 1-1: General rules and rules for buildings*. 2004.

[13] CEN (European Committee for Standardization), *Eurocode 1: Actions on structures - Part 1-1: General actions - Densities, self-weight, imposed loads for buildings*. 2002.

[14] CEN (European Committee for Standardization), *Eurocode - Basis of structural design*. 2002.

[15] SeismoSoft, "SeismoStruct 2021 - A computer program for static and dynamic nonlinear analysis of framed structures." 2021, [Online]. Available: http://www.seismosoft.com.

[16] R. Sousa, J. P. Almeida, A. A. Correia, and R. Pinho, "Shake table blind prediction tests: Contributions for improved fiber-based frame modelling," *J. Earthq. Eng.*, vol. 24, no. 9, pp. 1435–1476, 2020, doi: 10.1080/13632469.2018.1466743.

[17] M. A. Crisfield, "A consistent co-rotational formulation for non-linear, three-dimensional, beam-elements," *Comput. Methods Appl. Mech. Eng.*, vol. 81, no. 2, pp. 131–150, 1990, doi: 10.1016/0045-7825(90)90106-V.

[18] A. A. Correia and F. F. B. E. Virtuoso, "Nonlinear Analysis of Space Frames," in *Third European Conference on Computational Mechanics: Solids, Structures and Coupled Problems in Engineering*, 2006.

[19] J. B. Mander, M. J. N. Priestley, and R. Park, "Theoretical stress-strain model for confined concrete," *J. Struct. Eng.*, vol. 114, no. 8, pp. 1804–1825, 1988.

[20] M. Menegotto and P. Pinto, "Method of analysis for cyclically loaded R.C. plane frames including changes in geometry and non-elastic behavior of elements under combined normal force and bending," 1973.

[21] EC (European Commission - Research Fund for Coal and Steel), "Optimising the seismic performance of steel and steel-concrete structures by standardising material quality control," 2013.

[22] J. P. Almeida, D. Tarquini, and K. Beyer, "Modelling Approaches for Inelastic Behaviour of RC Walls: Multi-level Assessment and Dependability of Results," *Arch. Comput. Methods Eng.*, vol. 23, no. 1, pp. 69–100, 2016, doi: 10.1007/s11831-014-9131-y.

[23] A. Calabrese, J. P. Almeida, and R. Pinho, “Numerical issues in distributed inelasticity modeling of RC frame elements for seismic analysis,” *J. Earthq. Eng.*, vol. 14, no. SUPPL. 1, pp. 38–68, 2010, doi: 10.1080/13632461003651869.

[24] CEN (European Committee for Standardization), *Eurocode 8 — Design of structures for earthquake resistance - Part 3: Assessment and retrofitting of buildings*. 2005.